Geofenced Earthquake Notification System Using Haversine-Based Distance Calculation and MMI Intensity Estimation

Firdaus, S. R.,[1] Ahmad, U. A..[1*] Syauqi, F. B.,[1] Daryono,[2] Mustofa, F. C.,[3] Nugroho, H. A.,[4] Farady, I.[5] and Tresna, W. P.[6]
[1]School of Electrical Engineering, Telkom University, Indonesia
E-mail: sahrulfirdauz9987@gmail.com, umar@telkomuniversity.ac.id,* fasyaburhaniss@gmail.com
[2]Indonesia Defense University (UNHAN), Indonesia, E-mail: daryonobmkg@gmail.com
[3]The National Land Agency of Central Java Regional Office, Ministry of Agrarian Affairs and Spatial Planning (ATR-BPN), Indonesia, E-mail: fahmicmdw@stpn.ac.id
[4]State College of Meteorology, Climatology, and Geophysics (STMKG), Indonesia
E-mail: hapsoro.agung@stmkg.ac.id
[5]Department of Electrical Engineering, Yuan Ze University, Taiwan, E-mail: isackf@saturn.yzu.edu.tw
[6]Center for Photonics Research, National Research and Innovation Agency (BRIN), Indonesia
E-mail: wild004@brin.go.id
Corresponding Author

DOI: https://doi.org/10.52939/ijg.v22i8.5146

Abstract
Indonesia is one of the most seismically active countries in the world, making the rapid dissemination of official earthquake information essential for disaster mitigation and public situational awareness. This study presents the design and implementation of a mobile-based earthquake notification system that operates as a post-event notification platform by disseminating official earthquake information published by the Meteorology, Climatology, and Geophysical Agency (BMKG). The system is designed as an event-driven client–server architecture that brings together real-time earthquake data from BMKG, a Firebase-based cloud back-end, and Firebase Cloud Messaging (FCM). The notification mechanism uses the Haversine formula to determine the distance between the earthquake source and the user, while the Fukushima–Tanaka attenuation relationship is applied to estimate the corresponding ground motion. The resulting Peak Ground Acceleration (PGA) is then converted into Modified Mercalli Intensity (MMI). The felt intensity reported by BMKG serves as the reference threshold, which is subsequently used in a binary-search procedure to estimate the radius within which notifications should be delivered. Notifications are then selectively delivered only to users located within the estimated affected area. Experimental results show that the Haversine implementation achieved a Mean Absolute Error (MAE) of 0.0845 km, the proposed filtering mechanism correctly classified users according to the estimated notification radius, and the notification pipeline achieved average end-to-end latencies of 0.83 s and 1.87 s in foreground and background states, respectively. These results demonstrate that integrating geospatial proximity analysis with shaking-intensity estimation enables efficient and spatially relevant dissemination of official earthquake information while reducing unnecessary notifications to unaffected users. The proposed framework demonstrates that integrating geospatial proximity analysis with shaking-intensity estimation can improve the spatial relevance of post-earthquake notification dissemination.

Keywords: Android, Firebase Cloud Messaging, Geofencing, Haversine Formula, Mobile Earthquake Notification System, BMKG

1. Introduction

Indonesia is one of the most seismically active countries in the world because it is located at the convergence of the Australian, Eurasian, Pacific, and Philippine Sea tectonic plates. In addition, the country is crossed by numerous active fault systems and volcanic arcs, making earthquakes one of the most frequent natural hazards affecting the population [1] [2] and [3]. Earthquake events occur continuously throughout the year, with the Meteorology, Climatology, and Geophysics Agency

(BMKG) recording 43,439 earthquakes across Indonesia in 2025 alone, of which 973 were felt by the public and 25 caused structural damage [4]. This suggests that rapid and reliable dissemination of seismic information may play an important role in supporting disaster mitigation efforts and public situational awareness [5].

Official earthquake information in Indonesia is provided by the Meteorology, Climatology, and Geophysical Agency (BMKG) through the Indonesia Tsunami Early Warning System (InaTEWS) and several digital channels, most notably the official InfoBMKG mobile application, which delivers real-time earthquake data, felt-earthquake ("*Dirasakan*") reports, and notifications for earthquakes above magnitude 5.0 across the whole of Indonesia. The application issues a notification for every recorded earthquake event and does not provide users with an option to disable or customize these notifications, which has led users to report receiving repeated and, at times, excessive alerts within a short period [6]. This suggests that notifications are broadcast to users regardless of their distance from the affected area or their estimated exposure to the resulting shaking, rather than being tailored to individual recipients.

Addressing this limitation requires an approach capable of relating hazard information to the geographic context of individual users [7]. Recent developments in geoinformation have shown that spatial analysis is becoming an essential component of disaster risk management, as hazard information can be integrated with geographic characteristics to support more effective emergency response. Spatial vulnerability mapping enables disaster information to be interpreted according to the spatial distribution of exposed populations rather than through generalized regional descriptions. Similar geospatial approaches have been successfully applied for earthquake vulnerability assessment in Indonesia using GIS-based spatial analysis, demonstrating the importance of integrating geographic information into disaster mitigation strategies [8].

Several previous studies have investigated geospatial approaches for disaster-related applications. The Haversine formula has been widely adopted to calculate the shortest surface distance between two geographic coordinates and has demonstrated high accuracy for location-based services, including emergency-response and facility-locating applications [9][10] and [11]. Meanwhile, empirical ground-motion attenuation models have been developed to estimate Peak Ground Acceleration (PGA) [12], which can subsequently be converted into Modified Mercalli Intensity (MMI) for representing perceived ground shaking intensity [13] and [14]. Taken together, these studies show that geospatial distance calculations and ground-motion estimation can play an important role in earthquake-related applications. Most of the existing work, however, has concentrated on either measuring the distance to an earthquake source or characterizing the resulting ground motion. The integration of both approaches into a location-aware mobile system for delivering official earthquake information remains less explored.

At the same time, recent developments in earthquake information systems have increasingly combined mobile and geospatial technologies, opening new possibilities for delivering earthquake information to users in a more timely and location-specific manner. The MyShake platform combines smartphone-based seismic sensing, cloud processing, and mobile earthquake alert dissemination, demonstrating the feasibility of delivering earthquake information to geographically distributed smartphone users with low alert latency [15]. A subsequent implementation of the platform in California used estimated shaking intensity as a criterion for targeted alert delivery, with alerts directed to users within areas expected to experience MMI III or greater [16]. Taken together, these studies indicate that spatially targeted mobile alerts can improve the relevance of earthquake information by taking users' locations into account. Mobile applications have also been explored as practical interfaces for earthquake warning systems. For example, a mobile application integrated with the PRESTo earthquake early warning system demonstrated how smartphones can serve as operational interfaces for receiving alerts generated by an external seismic processing system [17]. Other research has examined the latency and geospatial accuracy of wireless emergency alerts associated with the ShakeAlert system, highlighting the importance of timely notification delivery and appropriate geographical targeting [7].

The reviewed literature, however, leaves a specific integration gap in the context of Indonesia. Existing studies do not appear to combine official BMKG earthquake information, user-to-epicenter distance calculation, attenuation-based estimation of the shaking radius, and selective post-event notification within a single mobile system. Most mobile earthquake warning platforms are designed for earthquake detection or early warning, whereas the system developed in this study operates after an earthquake event has been officially reported by BMKG. It is therefore not intended to independently detect earthquakes or replace BMKG's official assessment. Instead, the reported earthquake event and felt intensity provided by BMKG are used as the primary inputs. The system then estimates a spatial

ISSN: 1686-6576 (Printed) | ISSN 2673-0014 (Online) | © Geoinformatics International

notification boundary using Haversine-based distance calculation and a ground-motion attenuation relationship and delivers the information selectively to registered users located within the estimated affected area.

The contribution of this study is consequently centered on a location-aware post-event notification framework for disseminating official BMKG earthquake information according to users' geographic locations. The framework combines epicentral distance calculation based on the Haversine formula with Peak Ground Acceleration (PGA) estimation and Modified Mercalli Intensity (MMI) analysis to derive an approximate shaking-based notification radius. An event-driven cloud architecture integrates continuous earthquake-data acquisition, geospatial processing, Firebase-based data synchronization, and Firebase Cloud Messaging (FCM), allowing notifications to be generated and delivered with low latency. The framework was evaluated in terms of distance-calculation accuracy, shaking-radius estimation, selective notification performance, and end-to-end notification latency under both foreground and background application conditions. These experiments provide an integrated assessment of both the computational performance and operational behavior of the proposed location-aware earthquake notification system.

2. System Architecture and Method

2.1 System Architecture

From the perspective of geoinformation, the proposed framework functions as a spatial information system in which real-time seismic observations are transformed into location-aware geographic information products. The integration of spatial databases with operational services has been recognized as an effective approach for supporting spatial query processing and geospatial information management [18]. Building on this perspective, the system uses a client-server architecture that responds to events [19]. architecture consisting of four primary stages: data acquisition, data processing, data storage, and notification delivery. The proposed system adopts an event-driven client-server architecture consisting of four main stages: data acquisition, data processing, data storage, and notification delivery. Figure 1 illustrates the flow of earthquake information from BMKG to the mobile application and shows how user location data are incorporated into the notification process. As shown in Figure 1, the process begins when the back-end worker retrieves the latest earthquake and tsunami information published by BMKG. The worker is deployed on Google Compute Engine (GCE), which serves as the execution environment for the continuous back-end processes.

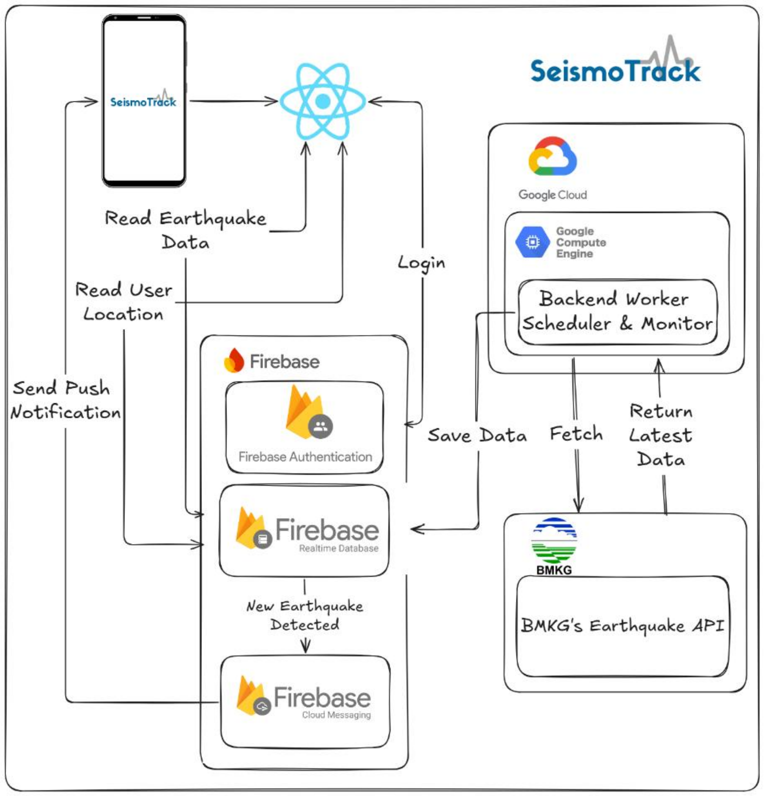

Figure 1 : Overall architecture of the proposed earthquake notification system

ISSN: 1686-6576 (Printed) | ISSN 2673-0014 (Online) | © Geoinformatics International

GCE is responsible for periodically retrieving earthquake data, processing incoming events, performing geospatial calculations, determining the estimated notification radius, and identifying users who satisfy the notification criteria. The processed earthquake information and registered user data are synchronized with Firebase Realtime Database, which acts as the central data storage layer. On the mobile side, users authenticate through Firebase Authentication, while the application periodically updates user-specific information, including geographic location, notification preferences, and Firebase Cloud Messaging (FCM) registration token.

Upon receiving a new earthquake event, the back-end calculates the epicentral distance for each registered user using the Haversine formula. It then estimates the corresponding shaking radius according to the attenuation-based method described in Section 2.3 and compares each user's location with the resulting spatial boundary. Users located within the estimated radius are selected as notification recipients, after which FCM delivers the earthquake information to their devices.

Thus, GCE functions as the computational back-end of the proposed architecture rather than as a data source. It separates continuous earthquake-data processing and notification logic from the mobile client, allowing the client to focus on user interaction, location updates, and notification presentation. Figure 1 therefore represents the complete processing flow from official earthquake data acquisition to location-aware notification delivery.

2.2 Distance Calculation Using the Haversine Formula

In geospatial applications, proximity analysis constitutes one of the fundamental spatial operations for supporting location-based services and geographic decision making. The computed distance serves as the basis for determining whether a geographic object is located inside or outside a dynamically defined spatial influence zone [20]. The distance between the earthquake epicenter and the user's location is calculated using the Haversine formula, which estimates the shortest distance between two geographic coordinates while considering the Earth's curvature [9][10] and [11]. The Haversine intermediate is defined in Equation 1:

$$a = \sin^2\left(\frac{\Delta\phi}{2}\right) + \cos(\phi_1)\cos(\phi_2)\sin^2\left(\frac{\Delta\lambda}{2}\right)$$

Equation 1

Where:

a = Haversine intermediate parameter

$Ø_1$ = latitude of the user

$Ø_2$ = latitude of the earthquake epicenter

$ΔØ$ = difference between the two latitudes

$\Delta\lambda$ = difference between the two longitudes

The surface distance is subsequently calculated as defined in Equation 2:

$$d = 2R \cdot \arcsin\sqrt{a}$$

Equation 2

Where:

R = mean Earth radius, set to 6,371 km in this study

d = great-circle distance between the user and earthquake epicenter in kilometres

Figure 2 summarizes this computation process, from the input coordinates through the calculation of the coordinate differences ($\Delta\varphi$, $\Delta\lambda$), the intermediate Haversine parameter a, and the resulting great-circle distance d between the user and the earthquake epicenter across Earth's surface (R = 6,371 km). The latitude and longitude differences are calculated from the corresponding coordinates of the user and the earthquake epicenter, while all angular coordinates are converted from degrees to radians before being substituted into Equation (1). The resulting distance represents the horizontal distance between the user and the earthquake epicenter and is subsequently used in the shaking-radius estimation described in Section 2.3.

2.3 Shaking radius estimation using PGA and MMI

The earthquake impact radius is estimated using the original Fukushima–Tanaka ground-motion attenuation relationship [12]. The proposed system estimates a notification radius by combining the horizontal distance obtained from the Haversine calculation, the earthquake focal depth, and an empirical ground-motion attenuation relationship. The estimated radius represents the distance at which the calculated ground shaking reaches the target MMI reported by BMKG. The effective hypocentral distance is first calculated as defined in Equation 3:

$$R_h = \sqrt{d^2 + h^2}$$

Equation 3

Where:

R_h = effective hypocentral distance in kilometres

h = the earthquake focal depth.

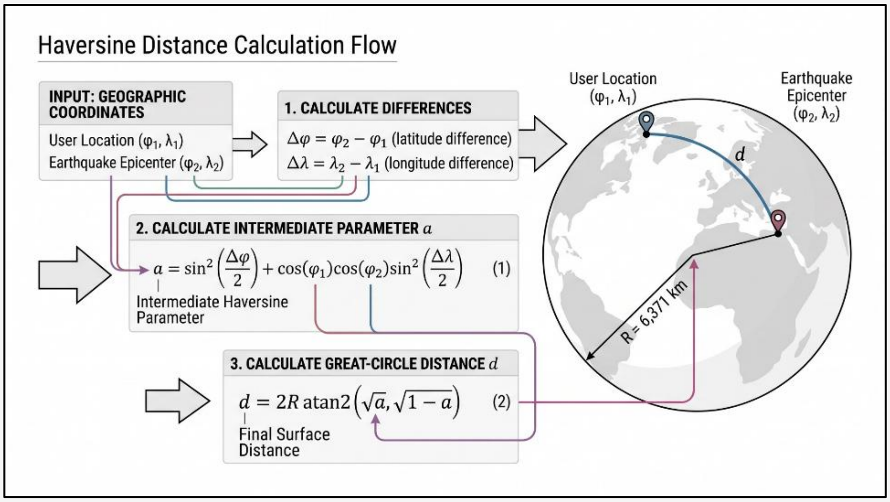

Figure 2 : Computation flow of the Haversine formula for estimating the great-circle distance between the user's location and the earthquake epicenter

Peak Ground Acceleration (PGA) is then estimated using the original Fukushima–Tanaka attenuation relationship [11], as defined in Equation 4:

$$\log_{10}(PGA) = 1.30 + 0.41M - \log_{10}\left(R_h + 0.032 \times 1010^{0.41M}\right) - 0.0034R_h$$

Equation 4

Where:

M = Earthquake magnitude

PGA = Estimated peak horizontal ground acceleration in cm/s^2 (Gal)

The empirical coefficients of the attenuation relationship are 1.30, 0.41, 0.032, and 0.0034 [12].

The original Fukushima–Tanaka model was developed from strong-motion records and expresses acceleration in cm/s^2. The original formulation uses the shortest distance between the recording site and the rupture surface as its distance parameter. In this study, the effective hypocentral distance calculated using Equation (3) is used as a simplified distance representation for estimating the notification radius. This simplification is intended for location-based filtering rather than for reproducing the physical ground-motion model. Accordingly, the resulting radius represents an empirical approximation of the area in which users are considered relevant recipients of the earthquake notification. The estimated PGA is subsequently converted into Modified Mercalli Intensity (MMI) using the empirical logarithmic relationship [13], as defined in Equation 5:

$$MMI = 3.66\log_{10}(PGA) - 1.66$$

Equation 5

Where:

MMI = estimated Modified Mercalli Intensity

The felt-intensity ("Dirasakan") data used as the target MMI in this study is obtained from BMKG's official earthquake information service, disseminated through the Indonesia Tsunami Early Warning System (InaTEWS) and its associated open-data portal [21]. For each earthquake assessed by BMKG as felt by the public, BMKG publishes a regional felt-intensity report expressed on the Roman-numeral Modified Mercalli Intensity (MMI) scale. The reported intensity is based on validated public felt reports collected through BMKG's observation network and is publicly accessible without authentication or subscription. In this study, the published BMKG intensity is treated as the official reference value, or target MMI, for the subsequent notification-radius estimation rather than being independently predicted by the proposed system. The Roman numeral intensity (e.g., II–III or III–IV) is first converted into its corresponding numeric MMI value by selecting the highest reported intensity level. A binary search procedure is then performed over increasing horizontal distances until the calculated MMI matches the official BMKG intensity. The corresponding distance is adopted as the notification radius. Based on the estimated MMI value at increasing distances from the epicenter, users are classified into two categories:

1. Affected, for users located inside the radius.
2. Safe, for users located outside the outer radius.

This estimation is intended solely for notification filtering and does not replace official shaking intensity assessments published by BMKG.

2.4 Selective Notification Delivery

The adoption of selective notification delivery in this study is motivated by two considerations: the operational limitation observed in the existing broadcast-based dissemination model, and empirical precedent from prior earthquake early-warning implementations demonstrating the benefits of targeted alert delivery.

As discussed in Section 1, the existing official notification channel disseminates an alert for every recorded event regardless of the recipient's distance from the epicenter or their exposure to the resulting ground shaking, a pattern that has been associated with users receiving alerts perceived as repeated and excessive [6]. This behavior is consistent with what warning-communication literature describes as *over-alerting*, in which high alert frequency combined with low message relevance leads recipients to disengage from, or opt out of, subsequent warnings [22]. Given that BMKG recorded tens of thousands of seismic events in a single year, of which only a small fraction was felt or damaging [4], sustaining a purely broadcast-based delivery model over time risks progressively eroding the perceived relevance and credibility of subsequent alerts, which is counterproductive to the goal of rapid and trustworthy information dissemination.

Selective delivery addresses this limitation by restricting notification dispatch to users whose estimated location falls within the shaking-affected radius derived in Section 2.3, rather than delivering every event to the entire user base indiscriminately. This design choice is further supported by precedent from operational earthquake early-warning systems: the MyShake platform's California implementation ties alert delivery to a minimum MMI threshold, restricting dissemination to users predicted to experience shaking at or above a defined intensity rather than notifying all registered users [22] and [23], and geofence-based testing conducted for the ShakeAlert Wireless Emergency Alert system specifically evaluated the effectiveness of confining alert delivery to a geographically defined target area, establishing geofencing as a recognized design pattern for reducing alert delivery outside the expected impact zone [5].

Accordingly, selective notification delivery is considered an appropriate approach for the objectives of this study, since it conditions the delivery decision on the estimated relevance of an event to each individual user rather than solely on the occurrence of a recorded earthquake. It should be noted, however, that the shaking radius used as the delivery criterion is derived from an attenuation relationship that has not been locally recalibrated for Indonesian seismotectonic conditions, so the resulting affected/safe classification carries some approximation error near the radius boundary (see Section 3.1 for the distance-calculation validation). Even with this limitation, filtering delivery by the estimated radius offers a more spatially relevant criterion than distributing every notification to the entire user base without location-based differentiation.

Building on the shaking radius and user classification established in the previous subsection, selective notification delivery is implemented using Firebase Cloud Messaging (FCM) together with Notifee for local notification rendering. Whenever a new earthquake event is synchronized, the back-end evaluates every registered user against three criteria:

1. The user is located within the estimated shaking radius.
2. A valid FCM registration token is available.
3. Notification permission has been granted

Only users satisfying all three conditions are included in the notification recipient list. On the client side, the mobile application processes incoming messages through a background notification handler capable of distinguishing between different alert categories. High-priority notifications are displayed using dedicated notification channels, sound, vibration, and application-launch behavior, allowing alerts to reach users regardless of whether the application is active or running in the background

3. Result and Discussion

3.1 Haversine Distance Calculation

The accuracy of the Haversine implementation was evaluated using 20 earthquake events obtained from official BMKG records. A fixed user coordinate of (-6.976, 107.635) was used throughout the experiment, while the epicenter coordinates were selected at random from recorded events. The calculated distances were compared against reference measurements obtained from Google Maps. As shown in Table 1, the proposed implementation achieved a Mean Absolute Error (MAE) of 0.0845 km across the 20 tested events, equivalent to approximately 84.5 m. The result indicates a high level of agreement between the calculated distances and the reference values, with most absolute errors

ISSN: 1686-6576 (Printed) | ISSN 2673-0014 (Online) |

below 0.10 km. The largest absolute error was observed at Point 2, with a deviation of 0.74 km from the reference distance of 1,530.04 km. Although this was the largest deviation among the tested points, the corresponding relative error was only approximately 0.048%, indicating that the difference was negligible in relation to the overall distance. The observed deviation can reasonably be attributed to differences in the distance models and coordinate precision used in the calculation and reference data. The Haversine formula assumes a spherical Earth with a constant mean radius of 6,371 km, whereas reference distances may be calculated using geodetic models such as WGS-84, which represents the Earth as an oblate spheroid. Differences may also arise from the coordinate precision of the earthquake epicenters reported by BMKG, particularly when latitude and longitude values are provided with limited decimal precision. In this study, the reference distances were obtained from Google Maps; consequently, their values may likewise depend on the coordinate precision entered into the mapping service and the underlying distance model used by the platform. Small differences in epicenter coordinates can produce increasingly noticeable distance differences over long baselines, which may contribute to the larger deviation observed at Point 2. Nevertheless, the overall MAE of 0.0845 km demonstrates that the Haversine implementation provides sufficiently accurate distance estimation for the location-based notification and geofencing requirements of the proposed system.

Table 1: Haversine distance calculation

No	Epicenter Coordinate (Lat, Lon)	System Output (km)	Reference Value (km)	Absolute Error (km)
1	-9.629, 119.421	1329.9	1329.7	0.2
2	-1.069, 120.116	1529.3	1530.04	0.74
3	-5.0198, 123.030	1716.2	1716.16	0.04
4	-6.839, 107.079	63.1	63.11	0.01
5	-5.439, 104.619	374.5	374.49	0.01
6	-1.139, 120.080	1524.8	1524.72	0.08
7	-3.730, 123.400	1782.0	1782.0	0.00
8	-1.079, 120.099	1529.7	1529.61	0.09
9	-7.410, 106.710	112.8	112.88	0.08
10	-3.929, 122.430	1672.1	1672.11	0.01
11	-2.839, 140.070	3621.5	3621.54	0.04
12	1.930, 127.390	2405.6	2405.58	0.02
13	-8.399, 116.199	957.0	956.97	0.03
14	2.040, 98.990	1387.7	1387.63	0.07
15	-5.429, 104.689	368.2	368.14	0.06
16	-9.609, 119.449	1332.4	1332.45	0.05
17	-2.329, 138.279	3434.2	3434.19	0.01
18	-7.529, 106.730	117.2	117.30	0.10
19	1.080, 120.920	1724.9	1724.89	0.01
20	-0.869, 127.480	2302.8	2302.76	0.04
MAE				0.0845

3.2 Shaking Radius Estimation

The shaking radius estimation was evaluated using five earthquake scenarios with different magnitudes and focal depths. For each event, the system estimated the Peak Ground Acceleration (PGA) using the Fukushima–Tanaka attenuation relationship and determined the notification radius corresponding to the Modified Mercalli Intensity (MMI) reported in the official BMKG earthquake bulletin. The results indicate that earthquake magnitude and focal depth significantly influence the estimated notification radius. In general, larger magnitude earthquakes produce wider notification areas, whereas shallower earthquakes generate stronger ground motion near the epicenter, resulting in larger radius for the same target intensity.

The MMI values used in this evaluation were obtained directly from official BMKG earthquake reports rather than estimated by the proposed system. Accordingly, the attenuation model was used only to determine the distance at which the calculated ground motion reached the reported MMI, and this distance was adopted as the notification radius. Figure 3 compares the notification radius generated by the proposed method with the official BMKG ShakeMap for the Berau earthquake event. The proposed system represents the potentially affected area as a circular geofence centered on the earthquake epicenter, whereas the BMKG ShakeMap depicts the spatial distribution of ground shaking based on instrumental observations and seismic analysis. The two representations therefore serve different purposes: the ShakeMap provides a spatially detailed representation of shaking intensity, while the proposed circular radius provides a simplified boundary for location-based notification filtering. Although the circular representation does not reproduce the spatial variability shown in the ShakeMap, it provides a practical approximation for identifying users within the estimated notification area.

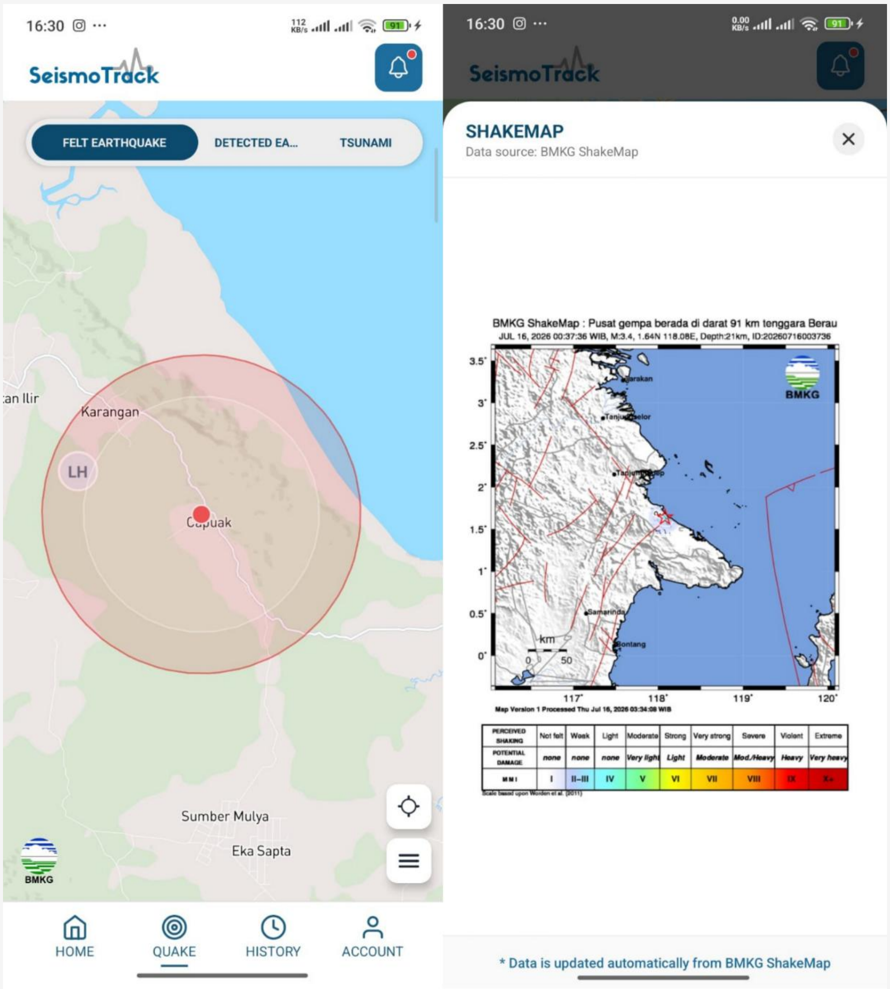

Figure 3 : Comparison between the estimated notification radius and the official BMKG ShakeMap for the Berau earthquake event

ISSN: 1686-6576 (Printed) | ISSN 2673-0014 (Online) | © Geoinformatics International

Table 2: Shaking radius estimation

No	Magnitude	Depth (km)	MMI	PGA (Gal)	Radius (km)	Location
1	3.4	21	3	19.22	4.51	Berau
2	2.8	5	3	48.58	12.06	East Kolaka
3	5.4	10	4	197.46	54.15	Buol
4	4.1	12	3	64.16	34.72	Jembrana
5	7.7	47	6	213.27	63.28	Karatung Island
6	4.4	2	3	292.13	45.38	Sigi
7	4.5	17	3	63.42	45.56	Konawe Sea
8	3.2	26	2	12.51	17.53	Sukabumi
9	7.7	15	6	23.85	10.70	Nagekeo
10	4.4	29	4	89.28	76.22	Parigi Moutong

From a geoinformation perspective, the objective of the proposed model is not to reproduce the detailed spatial distribution of ground shaking but to provide an efficient geographic approximation for prioritizing emergency notifications. This approach is consistent with previous geospatial disaster studies, where simplified spatial models have been employed to support disaster mitigation and emergency response planning rather than to replicate the underlying physical processes with seismological precision [8]. Finally, it should be noted that the Fukushima–Tanaka attenuation relationship was originally developed using Japanese strong-motion records [12]. Consequently, the notification radius presented in Table 2 should be interpreted as approximations derived from this empirical attenuation model rather than as replacements for BMKG's official ShakeMap products. Comprehensive validation using a larger set of Indonesian earthquake events covering diverse tectonic environments would be required to further assess the applicability of the model for nationwide deployment.

3.3 Selective Notification Delivery

The selective notification mechanism was validated using five representative user locations corresponding to different distances from the earthquake epicenter. The validation was conducted using the Berau earthquake (coordinates: 1.64°N, 118.08°E) that occurred on 13 July 2026 (Table 3). The results indicate that the proposed filtering algorithm correctly determined notification recipients according to the estimated shaking radius [7]. Users located within the affected area received earthquake notifications, whereas users outside the estimated shaking radius did not receive any alerts. These findings indicate that the proposed geofencing approach can effectively limit notification delivery to users within the estimated notification area. By combining geospatial filtering with mobile information services, the system improves the spatial relevance of earthquake-related communication without requiring notifications to be sent to all registered users. Instead, notifications are directed to users whose locations fall within the estimated radius, providing a more targeted and location-specific means of disseminating official earthquake information.

3.4 Notification Latency

To evaluate the performance of the notification pipeline, 146 controlled experiments were conducted, consisting of 81 foreground tests and 65 background tests. Notification latency was measured as the elapsed time between payload generation on the back-end and notification rendering on the Android device. Figure 4 End-to-end notification latency in foreground and background states the proposed system achieved an average notification latency of 0.83 seconds in the foreground state and 1.87 seconds in the background state. The background measurements exhibited greater variability, with a maximum latency of 3.72 seconds, primarily due to Android operating system resource management and battery optimization mechanisms. (Figure 5).

Table 3: Selective notification delivery

No	User Coordinate (Lat, Lon)	Distance to Epicenter (km)	Zone Classification (km)	Notification Received
1	-6.976, 107.635	1503.8	Safe	No
2	-1.648,118.047	3.7	Affected	Yes
3	-6.950,106.933	1562.8	Safe	No
4	1.636, 118.070	1.1	Affected	Yes
5	1.647, 118.057	2.7	Affected	Yes

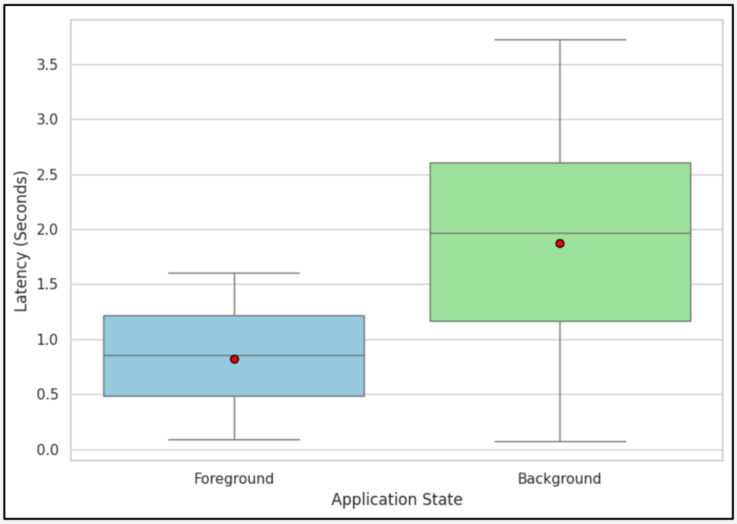

Figure 4: End-to-end notification latency in foreground and background states

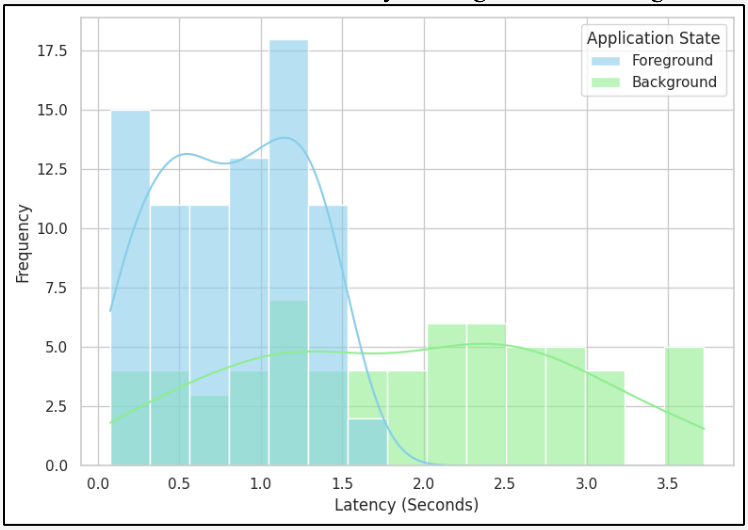

Figure 5: Distribution of notification latency

The latency distribution indicates that foreground notifications were generally delivered faster and with less variability than background notifications, consistent with differences in how the Android operating system schedules and manages background processes [24][25] and [26]. Overall, the experimental results indicate that the proposed event-driven architecture provides timely dissemination of official earthquake information while maintaining selective notification delivery based on user location.

3.5 Mobile Application Interface

The developed mobile application provides an adaptive user interface that presents earthquake information according to the user's estimated hazard status (Figure 6).

ISSN: 1686-6576 (Printed) | ISSN 2673-0014 (Online) | © Geoinformatics International

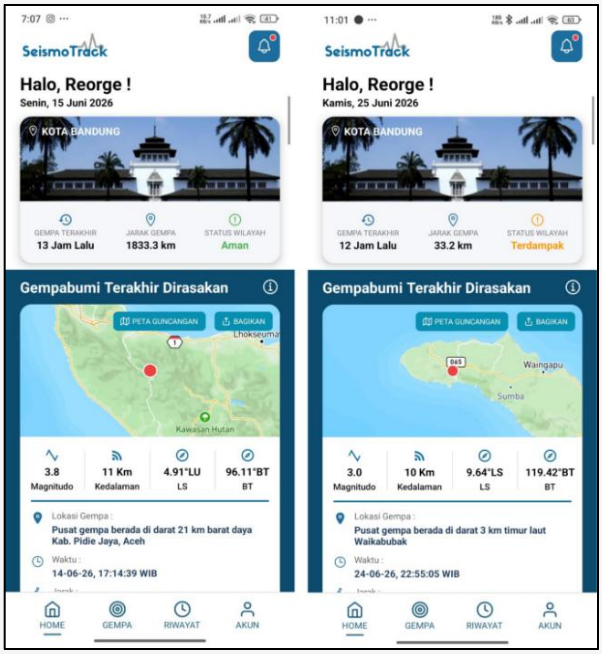

Figure 5 : Mobile interface under different hazard conditions

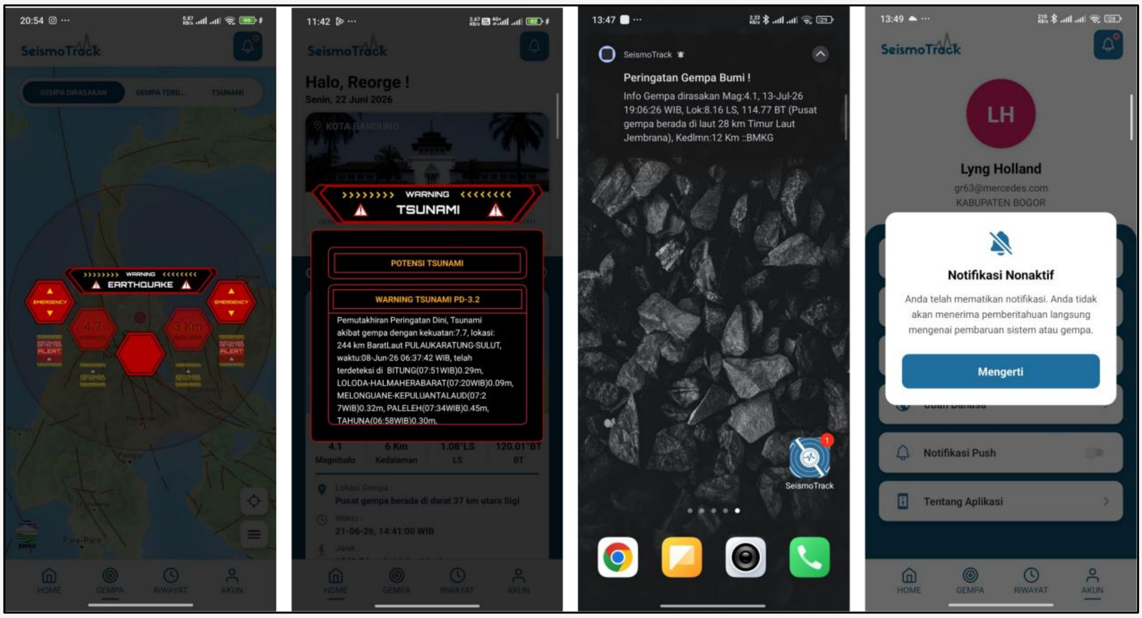

Figure 7: Foreground and background notification interface

The interface dynamically changes according to the user's position relative to the estimated shaking radius, allowing users to identify whether they are categorized as affected or safe. Real-time earthquake information, including magnitude, depth, and distance to the epicenter, is presented together with visual indicators intended to support situational awareness (Figure 7). The notification interface supports both foreground and background application states and distinguishes between earthquake and tsunami alerts through separate visual and audio cues. During foreground execution, a dedicated emergency overlay immediately presents essential earthquake or tsunami information, with tsunami alerts displayed using distinct color coding and iconography to reflect their higher urgency. When the application is running in the background, high-priority push notifications accompanied by sound and vibration deliver disaster information without requiring the application to remain open.

In contrast to existing platforms such as InfoBMKG, which does not provide users with an option to disable or customize notifications [6], the proposed application includes a toggle setting that allows users to enable or disable each notification category individually, addressing user complaints regarding uncontrollable and repeated alerts.

3.6 Limitations of the Proposed Approach

Several limitations should be considered when interpreting these results. First, the number of test cases was not the same across the evaluated components. The Haversine distance calculation was tested using 20 earthquake events, whereas the shaking-radius estimation and selective notification delivery were evaluated using 10 and 5 cases, respectively. These experiments provide evidence of the functional consistency of the proposed approach, but the datasets remain relatively small compared with the range of earthquake characteristics and geographic conditions found across Indonesia. A larger and more diverse set of events would therefore be needed to assess the generalizability of the findings more robustly.

Second, the estimated shaking radius is based on the Fukushima–Tanaka ground-motion attenuation relationship, which was originally developed from Japanese strong-motion records and has not been specifically calibrated to Indonesia's seismotectonic conditions. The resulting radius was qualitatively compared with the official BMKG ShakeMap for one representative earthquake event (Section 3.2, Figure 2). However, the study did not perform a quantitative, event-by-event spatial comparison across multiple earthquakes. The extent to which the attenuation-based radius represents actual shaking patterns under different Indonesian earthquake conditions therefore remains to be established.

Third, the proposed system uses the officially reported BMKG felt intensity (“Dirasakan”) as the target MMI rather than estimating shaking intensity independently from raw instrumental data. The accuracy and timeliness of the resulting notification radius are consequently influenced by the coverage and reporting latency of BMKG's felt-report network. These factors may vary between regions, particularly where population density and observation infrastructure differ substantially.

Fourth, the proposed system's operational reliability is bounded by two external dependencies beyond its control. On the delivery side, notification receipt requires an active internet connection on the recipient's device; users without connectivity at the time of an event will not receive an alert regardless of their classified hazard status. On the acquisition side, the back-end worker retrieves earthquake information by periodically polling BMKG's open-data feed rather than receiving a direct push from BMKG; consequently, the end-to-end notification latency reported in Section 3.4 reflects only the system's internal processing and delivery time, and does not account for any additional delay introduced by BMKG's own data-publishing latency or feed availability.

Finally, while the notification pipeline was evaluated for delivery latency (Section 3.4) and the interface was validated in terms of functional behavior (Section 3.5), the perceived relevance and usability of selective notification delivery from an end-user perspective was not evaluated through a formal user study. This aspect, along with the development of a locally calibrated attenuation model, is addressed as future work in the following section.

4. Conclusion

This study aimed to address the limitations of conventional broadcast-based emergency alerts by designing and implementing a location-aware, mobile-based earthquake notification system capable of selectively disseminating official information from the Meteorology, Climatology, and Geophysics Agency (BMKG). To achieve this objective, the research integrated an event-driven cloud architecture with Haversine-based distance calculations and the Fukushima–Tanaka ground-motion attenuation relationship. This approach enabled the system to dynamically estimate Peak Ground Acceleration (PGA) and determine a precise notification radius corresponding to the official target Modified Mercalli Intensity (MMI) via a binary search procedure. The synthesized experimental results confirm that the proposed framework consistently met its technical and operational goals. Specifically, the Haversine-based proximity analysis achieved a Mean Absolute Error (MAE) of 0.0845 km, providing highly accurate geofencing boundaries. Consequently, the spatial filtering mechanism successfully restricted notification delivery strictly to users located within the estimated shaking impact area, effectively mitigating the risk of warning fatigue among unaffected populations. Furthermore, the notification pipeline demonstrated rapid responsiveness, recording average end-to-end delivery latencies of 0.83 seconds in the foreground state and 1.87 seconds in the background state. Alongside these performance metrics, the mobile application successfully empowered users with granular control over their disaster alerts by distinguishing between earthquake and tsunami events through independent notification toggles. The broader implication of these findings is that the integration of real-time seismic observations, spatial database management, and geographic proximity analysis can significantly enhance operational disaster management and spatial decision support systems. By transitioning from a generalized broadcast model to a targeted, location-based information service, the framework provides a practical solution for modern disaster mitigation. Nevertheless, these contributions must be contextualized within the study's current limitations. The empirical attenuation model utilized has not yet been calibrated specifically for Indonesia’s diverse seismotectonic environment, and the hazard zone is represented by a simplified circular geofence rather than an asymmetric shaking pattern reflecting localized geological conditions. Furthermore, the system requires comprehensive end-user evaluation. Therefore, future work will prioritize developing region-specific attenuation models, implementing asymmetrical geofencing algorithms, and conducting systematic usability assessments with a larger demographic to optimize the platform's operational reliability and public acceptance.

Acknowledgement

The authors gratefully acknowledge Telkom University for the APC support provided for the publication. Sincere gratitude is also extended to BMKG of Indonesia for the provision of the open-access seismic data and operational parameters, which were crucial for the system's heuristic modeling and real-time evaluation.

References

[1] Kusworo, K. and Tjenreng, Z., (2025). Analysis of Government Policy Implementation in Natural Disaster Management through National Search and Rescue (SAR) In Indonesia. *Jurnal Ilmu Pemerintahan: Kajian Ilmu Pemerintahan dan Politik Daerah*, Vol. 10(2), 154–163. https://doi.org/10.24905/jip.10.2.2025.154-163.

[2] Kinasih, F. A., Miladan, N. and Kusumastuti, K., (2023). Kajian risiko bencana gempa bumi akibat aktivitas Sesar Lembang di Kabupaten Bandung Barat [Study of Earthquake Disaster Risk due to Lembang Fault Activity in West Bandung Regency]. *Region: Jurnal Pembangunan Wilayah dan Perencanaan Partisipatif,* Vol. 18(2). https://doi.org/10.20961/region.v18i2.57232.

[3] Usiono, D. A. Putri, N., Hasanah and Purba, T. P. B., (2024). Mini Research on Earthquake Alert at Jumbara PMI. *AMK: Abdi Masyarakat UIKA*, Vol. 3(1). 1–5. https://doi.org/10.32832/amk.v3i1.2137.

[4] Sef, "Waspada Warga RI, 43.439 Gempa Terjadi Sepanjang, (2025). *CNBC Indonesia, Jan. 2, 2026.* [Online]. Available: https://www.cnbcindonesia.com/news/20260102063203-4-698995/waspada-warga-ri-43439-gempa-terjadi-sepanjang-2025. [Accessed: Jul. 13, 2026].

[5] Pierleoni, P., Concetti, R., Belli, A., Palma, L., Marzorati, S. and Esposito, M., (2023). A Cloud-IoT Architecture for Latency-Aware Localization in Earthquake Early Warning. *Sensors*, Vol. 23(20). https://doi.org/10.3390/s23208431.

[6] Kirby, L., Tolle, H. and Brata, A. H., (2019). Perancangan User Experience Aplikasi Mobile Social Crowdsourcing Bencana Alam menggunakan Pendekatan Human-Centered Design (HCD) [User Experience Design of Natural Disaster Mobile Social Crowdsourcing Application Using Human-Centered Design (HCD) Approach]. *Jurnal Pengembangan Teknologi Informasi dan Ilmu Komputer,* Vol. 3(5); 4702–4709. http://j-ptiik.ub.ac.id/index.php/j-ptiik/article/view/5318.

[7] McBride, S. K., Sumy, D. F., Llenos, A. L., Parker, G. A., McGuire, J., Saunders, J. K., Meier, M. A., Schuback, P., Given, D. and de Groot, R., (2023). Latency and Geofence Testing of Wireless Emergency Alerts Intended for the ShakeAlert® Earthquake Early Warning System for the West Coast of the United States of America. *Safety Science,* Vol. 157. https://doi.org/10.1016/j.ssci.2022.105898by.

[8] Pamungkas, T. D., Ningrum, E., Arrasyid, R., Aliyan, S. A., Firdaus, R. A., Syaripah, G. K., Fikri, H. and Ayesha, P. A., (2026). Earthquake Vulnerability Mapping Using Spatial and SWOT Analysis: A Case Study at Cisarua, Indonesia. *International Journal of Geoinformatics*, Vol. 22(5), 59–71. https://doi.org/10.52939/ijg.v22i5.4980.

[9] Basyir, M., Nasir, M., Suryati, S. and Mellyssa, W., (2018). Determination of Nearest Emergency Service Office Using Haversine Formula Based on Android Platform. *EMITTER International Journal of Engineering Technology*, Vol. 5(2), 270–278. https://doi.org/10.24003/emitter.v5i2.220.

[10] Maria, E., Budiman, E., Haviluddin, and Taruk, M., (2020). Measure Distance Locating Nearest Public Facilities Using Haversine and Euclidean Methods. *Journal of Physics: Conference Series*, Vol. 1450(1). https://doi.org/10.1088/1742-6596/1450/1/012080.

[11] Tundjungsari, V., (2025). Development of Location-Based Emergency Mobile Application During Disaster with Haversine Formula and QGIS. *Technovasia: Journal of Technology & Computer Research in Innovation, Science, and Applications*, Vol. 1(1), 48–56. Available: https://journal-iam.com /index.php/technovasia/article/view/28.

[12] Fukushima, Y. and Tanaka, T., (1990). A New Attenuation Relation for Peak Horizontal Acceleration of Strong Earthquake Ground Motion in Japan. *Bulletin of the Seismological Society of America*, Vol. 80(4), 757–783.

[13] Wald, D. J., Quitoriano, V., Heaton, T. H. and Kanamori, H., (1999). Relationships Between Peak Ground Acceleration, Peak Ground Velocity, and Modified Mercalli Intensity in California. *Earthquake Spectra*, Vol. 15(3), 557–564. https://doi.org/10.1193/1.1586058.

[14] Pasau, G., Tamuntuan, G. H., Tanauma, A., Pandara, D. P., Ferdy, A. F., As'ari, and Maramis, C., (2021). Empirical Attenuation Model for Predicting Peak Ground Acceleration in North Arm Sulawesi, Indonesia. *IOP Conference Series: Materials Science and Engineering*, Vol. 1115(1). https://doi.org/10. 1088/1757-899X/1115/1/012069.

[15] Allen, R. M., Kong, Q. and Martin-Short, R., (2020). The MyShake Platform: A Global Vision for Earthquake Early Warning. *Pure and Applied Geophysics,* Vol. 177, 1699–1712. https://doi.org/10.1007/s00024-019-02337-7.

[16] Strauss, J. A., Kong, Q., Pothan, S., Thompson, S., Mejia, R. F., Allen, S., Patel, S. and Allen, R. M., (2020). MyShake Citizen Seismologists Help Launch Dual-Use Seismic Network in California. *Frontiers in Communication,* Vol. 5. https://doi.org/10.3389/fcomm.2020.00032.

[17] Satriano, G. P., Picozzi, M., Zollo, A., Caruso, S. and Minielly, G., (2020). Design and Implementation of a Mobile Device App for Network-Based Earthquake Early Warning Systems (EEWSs): Application to the PRESTo EEWS in southern Italy. *Natural Hazards and Earth System Sciences,* Vol. 20, 921–936.

[18] Budisusanto, Y., Azhar, M., Alawi, A. and Mushthofa, A., (2026). Design and Implementation of Land Information System Using Spatial Database. *International Journal of Geoinformatics*, Vol. 22(5), 127–143. https://doi.org/10.52939/ijg.v22i5.4983.

[19] Kokal, N., (2025). Event-Driven Architectures for Ultra-Low-Latency Systems: Design Principles, Reference Patterns, and Evaluation. *International Journal of Computational and Experimental Science and Engineering*, Vol. 11, 1–15. https://doi.org/10.22399/ijcesen.4303.

[20] Kurniawan, B. A., Mumpuni, R. and Al Haromainy, M. M., (2025). Design and Development of a Real-Time Delivery Tracking App Using WebSocket and Haversin. *Bit-Tech*, Vol. 8(2), 2482–2494.

[21] Badan Meteorologi, Klimatologi, dan Geofisika, (BMKG). (2026). *Indonesia Tsunami Early Warning System* (InaTEWS). InaTEWS. [Online]. Available: https://inatews.bmkg.go.id [Accessed: Jul. 13, 2026].

[22] Sutton, J. and Wood, M. M., (2025). Opting Out: Over-Alerting and Warning Fatigue in the Era of Wireless Emergency Alerts. *Journal of Contingencies and Crisis Management,* Vol. 33(3). https://doi.org/10.1111/1468-5973.700 76.

[23] Strauss, J. A., Kong, Q., Pothan, S., Thompson, S., Mejia, R. F., Allen, S., Patel, S. and Allen, R. M., (2020). MyShake Citizen Seismologists Help Launch Dual-Use Seismic Network in California. *Frontiers in Communication,* Vol. 5. https://doi.org/10.3389/fcomm.2020.00032.

[24] González-Pérez, A., Matey-Sanz, M., Granell, C. and Casteleyn, S., (2022). Using Mobile Devices as Scientific Measurement Instruments: Reliable Android Task Scheduling. *Pervasive and Mobile Computing*, Vol. 81. https://doi.org/10.1016/j.pmcj.2022.101550.

[25] Hahn, S. S., Lee, S., Yee, I., Ryu, D. and Kim, J., (2017). Improving User Experience of Android Smartphones Using Foreground App-Aware I/O Management. *Proceedings of the 8th ACM SIGOPS Asia-Pacific Workshop on Systems (APSys '17)*. https://doi.org/10.1145/31 24680.3124721.

[26] Sutter, T., (2019). *Simple Spyware Androids Invisible Foreground Services and How to (Ab)use Them.* Whitepaper, Zurich University of Applied Sciences, Winterthur, Switzerland.